Observed effects of solar proton events and sudden stratospheric warmings on odd nitrogen and ozone in the polar middle atmosphere

S.-M. Päivärinta,[1] A. Seppälä,[1] M. E. Andersson,[1] P. T. Verronen,[1] L. Thölix,[1] and E. Kyrölä[1]

Received 14 December 2012; revised 10 May 2013; accepted 11 May 2013; published 26 June 2013.

[1] Here we use satellite observations from the ACE-FTS, MLS/Aura and SABER/TIMED to study the effects of solar proton events (SPEs) and strong sudden stratospheric warmings (SSWs) on the middle atmospheric odd nitrogen (NO_x) and ozone levels in the Northern Hemispheric polar region. Three winters (January–March) are considered: (1) 2005 (SPE), (2) 2009 (SSW), and (3) 2012 (SPEs and SSW). These different cases provide a good opportunity to study the roles that transport from the mesosphere-lower thermosphere region and in situ production due to particle precipitation have on stratospheric NO_x levels and the consequent effects on the middle atmospheric ozone. The observations show increases in NO_x after both the SPEs (days to weeks) and SSWs (weeks to months) by up to a factor of 25 between 40 and 90 km. The largest mesospheric NO_x increases are observed following the SSW in late January 2009, but the most substantial effects in the upper stratosphere are seen when both an SSW and in situ production by SPEs take place (2012), even though the in situ NO_x production in 2012 was relatively weak in magnitude compared to periods of much higher solar activity. In 2012, both short-term (days, due to SPEs and odd hydrogen) depletion and longer-term (months, due to several drivers) depletion of ozone of up to 90% are observed in the mesosphere and upper stratosphere, coinciding with the enhanced amounts of NO_x.

Citation: Päivärinta, S.-M., A. Seppälä, M. E. Andersson, P. T. Verronen, L. Thölix, and E. Kyrölä (2013), Observed effects of solar proton events and sudden stratospheric warmings on odd nitrogen and ozone in the polar middle atmosphere, *J. Geophys. Res. Atmos.*, *118*, 6837–6848, doi:10.1002/jgrd.50486.

1. Introduction

[2] Odd nitrogen ($NO_x = N + NO + NO_2$) is constantly produced in the lower thermosphere by solar EUV (extreme ultraviolet) radiation, soft X-rays, and energetic particles, i.e., auroral electrons [*Barth*, 1992]. In polar winter, in the absence of solar radiation, the chemical lifetime of NO_x is long and therefore the upper atmospheric NO_x can be transported inside the polar vortex to the middle atmosphere. *Solomon et al*. [1982] showed that if the descent continues down to stratospheric altitudes, NO_x can have an effect not only on the stratospheric NO_x amounts but also on ozone by destruction in catalytic chemical cycles. Mesospheric production of NO_x by energetic particle precipitation (proton and electron precipitation) can have an important role in intensifying the mesosphere-lower thermosphere (MLT) to stratosphere NO_x connection since the downward transport of thermospheric air masses through the mesopause (at ~90–100 km) is hindered by the wintertime upper atmospheric circulation patterns [*Smith et al*., 2011]. Stratospheric conditions are known to have an influence on the troposphere through top-down coupling [*Baldwin and Dunkerton*, 2001], and it has recently been suggested that changes in mesospheric-stratospheric NO_x and ozone concentrations could modulate the polar surface air temperatures by affecting the radiative budget and, through that, atmospheric circulation patterns [*Seppälä et al*., 2009; *Baumgaertner et al*., 2011].

[3] *Callis et al*. [1991a] studied the link between energetic particle precipitation, especially electrons, and stratospheric NO_x and ozone. They used satellite observations and a two-dimensional model to show that a connection between energetic particle precipitation and the middle and lower atmosphere exists. Further studies [e.g., *Callis et al*., 1991b; *Callis et al*., 1996a, 1996b; *Callis*, 1997; *Callis and Lambeth*, 1998] gave some indication that electron precipitation can, in fact, provide a significant source of NO_x between the upper stratosphere and mesosphere and that significant amounts of stratospheric ozone can be destroyed due to the enhanced NO_x concentrations. However, no strong conclusions on the long-term effects could be made due to scarcity of the observations.

[4] The NO_x connection between the MLT and stratosphere can be intensified by solar proton events (SPEs) and sudden stratospheric warmings (SSWs). SPEs are caused by

[1]Earth Observation Finnish Meteorological Institute, Helsinki, Finland.

Corresponding author: S.-M. Päivärinta, Earth Observation, Finnish Meteorological Institute, PO Box 503, Helsinki 00280, Finland. (sanna-mari.paivarinta@fmi.fi)

2169-897X/13/10.1002/jgrd.50486

large eruptions like coronal mass ejections in the Sun. During these eruptions, protons and heavier ions are emitted from the Sun and, when directed toward the Earth, are guided by the Earth's magnetic field to the polar regions where they precipitate into the atmosphere. SPEs occur on a sporadic basis but are more frequent during periods near solar maximum [*Jackman et al*., 2009]. SPEs have a direct effect in the mesosphere and stratosphere where they produce NO_x and odd hydrogen ($HO_x = H + OH + HO_2$) in situ through dissociation and dissociative ionization of neutral molecules (primarily N_2) in the atmosphere [e.g., *Jackman et al*., 2000; *López-Puertas et al*., 2005; *Seppälä et al*., 2004; *Verronen et al*., 2005; *Jackman et al*., 2008; *Seppälä et al*., 2008]. For example, the Halloween 2003 SPEs increased NO_x concentrations by an order of magnitude above 40 km, which lead to an ozone decrease of 20–60% over a period of several weeks [*Seppälä et al*., 2004]. Depending on the season, NO_x produced by the SPEs may influence the middle atmospheric chemistry for months or even years [*Jackman et al*., 2009]. SSWs, on the other hand, can intensify the downward transportation of NO_x from the MLT region to the stratosphere. Sudden stratospheric warming events are caused by vertically propagating planetary waves interacting with the zonal winds, leading to the breakdown or displacement of the polar vortex [*Matsuno*, 1971]. SSW events mainly occur in the Northern Hemisphere (NH) due to larger planetary wave activity. On average, an SSW event takes place about once every other winter. When the stratopause reforms after the SSW event, a period of strong downward transport of mesospheric and upper stratospheric air can take place, intensifying the descent inside the polar vortex.

[5] Several previous studies have discussed the MLT to stratosphere descent of NO_x and the possible influence on stratospheric ozone [e.g., *Funke et al*., 2005; *Randall et al*., 2006, 2009; *Funke et al*., 2011; *Salmi et al*., 2011; *von Clarmann et al*., 2013], but the roles of SPEs and SSWs as an NO_x source are still unclear. In the NH, NO_x descent events have been reported for early 2004, 2006, and 2009 [*Randall et al*., 2006, 2009]. Simultaneous ozone loss due to NO_x chemistry has been reported for the 2004 case [e.g., *Randall et al*., 2005; *Clilverd et al*., 2006, 2009]. The large NO_x amounts in the middle atmosphere in 2004 were most likely a result of the combined effects of increased particle precipitation from the massive SPEs in late 2003 and electron precipitation in early 2004 [*Clilverd et al*., 2009; *Semeniuk et al*., 2005] and the strong dynamical events following the December 2003 SSW [*Funke et al*., 2007; *Hauchecorne et al*., 2007].

[6] The aim of this investigation is to study the effects of SPEs and SSWs on middle atmospheric NO_x and ozone using satellite observations from the ACE-FTS, MLS/Aura, and SABER/TIMED. For our analysis, we have chosen the events that took place early in the years 2005, 2009, and 2012 because of their different characteristics: (1) SPEs occurred in 2005 and 2012 and (2) SSWs in 2009 and 2012. Other studies have also previously discussed the years 2005 (one SPE) [e.g., *Seppälä et al*., 2006; *Jackman et al*., 2011] and 2009 (a SSW event) [e.g., *Randall et al*., 2009; *Salmi et al*., 2011], and recently, *von Clarmann et al*. [2013] reported atmospheric responses to the 2012 SPEs. In this study we will contrast these three years with very different conditions while providing additional attention to year 2012, as this was a special case when several SPEs and a SSW took place, providing optimal conditions for the NO_x connection between MLT and the stratosphere to occur.

2. Data Description

2.1. ACE-FTS

[7] The ACE (Atmospheric Chemistry Experiment) satellite is a Canadian-led mission and was launched into low Earth circular orbit in 2003 [*Bernath et al*., 2005]. The satellite, also known as SCISAT-1, carries two instruments: FTS (Fourier Transform Spectrometer) and MAESTRO (Measurement of Aerosol Extinction in the Stratosphere and Troposphere Retrieved by Occultation). The FTS instrument is the primary instrument of the satellite and provides the main data (NO_x and O_3) used in this study. The ACE-FTS is a high spectral resolution instrument measuring the vertical distribution of trace gases and temperature. The measurements are carried out during sunset and sunrise, leading to a limited latitudinal coverage (Figure 1). The vertical resolution is about 4 km, covering the altitude range from the cloud tops up to about 150 km. We do not use any observations from the Southern Hemispheric polar region for this study as the number of observations in that area was very low during our study periods. In our analysis, we combined sunrise and sunset data neglecting possible NO_x asymmetry due to nighttime N_2O_5 buildup. However, this should make no significant impact on our results, because we only consider altitudes above 35 km where the N_2O_5 amounts are typically only a small fraction of those of NO_x.

[8] Measurement errors for NO_x vary with altitude and time. Below 25 km, the errors are over $\pm$40% and are hence not used. Between 25 and 45 km, the errors are quite small ($<$20%) but increase above 45 km ($>$20%). For NO and NO_2 separately, the errors are generally below 30% and 4–20% at around 50 km, respectively. The NO measurements become more unreliable with increasing altitude. For ozone, the errors are below 5% between 10–65 km and 85–95 km but can increase to $>$100% between these two regions (75–85 km).

2.2. MLS

[9] The Microwave Limb Sounder (MLS) instrument on board NASA's EOS Aura satellite was launched in 2004 and placed into a Sun-synchronous orbit at about 705 km altitude [*Waters et al*., 2006]. MLS observes thermal microwave emissions, scanning from the ground to 90 km every 25 s with daily global coverage of about 13 orbits per day. In this study, we use Version 3.3 Level 2 daily geopotential height (GPH), daily CO, and nighttime O_3 (solar zenith angles $>100°$), all screened according to the MLS data description and quality document [*Livesey et al*., 2011]. Details on validation of the MLS GPH, CO, and O_3 are given in *Schwartz et al*. [2008], *Pumphrey et al*. [2007], and *Jiang et al*. [2007], respectively. The vertical resolution of the MLS ozone measurements is about 2–3 km from the upper troposphere (12 km) to the middle mesosphere (65 km) and about 5 km above 65 km [*Jiang et al*., 2007]. The latitudinal coverage is 82°S–82°N, enabling the use of MLS data to look for hemispheric differences. The standard error of the mean for the MLS ozone data used in this study is, on average, $<$10% below 60 km and 10–20% above.

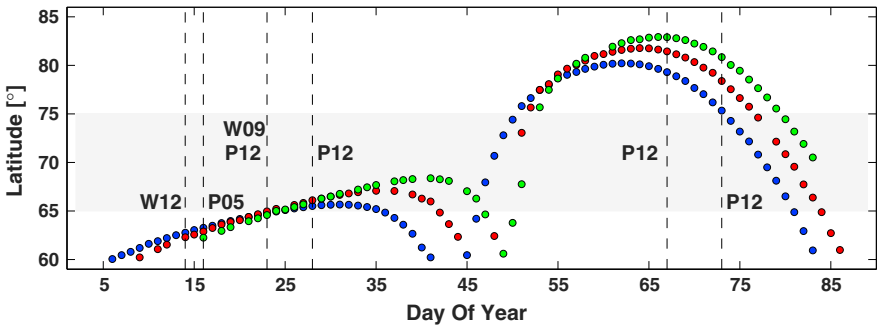

Figure 1. Daily averages of ACE-FTS measurement latitudes in January–March 2005 (blue), 2009 (red), and 2012 (green). The latitude range (65°N–75°N) used in the analysis of SABER and MLS measurements is marked in the figure with gray shading. The vertical dashed lines show the time points for SPEs (P) and SSWs (W) during 2005 (05), 2009 (09), and 2012 (12).

2.3. SABER

[10] SABER (Sounding of the Atmosphere using Broadband Emission Radiometry) is a 10-channel limb-scanning radiometer flying on NASA's TIMED satellite launched in 2002 [*Russell et al*., 1999]. SABER scans the Earth's limb from 400 km tangent height to the ground, simultaneously recording profiles of radiance in the spectral range from 1.27 to 15.4 μm [*Mlynczak et al*., 2005]. The instrument records approximately 1600 profiles per day. In this study we use the SABER (v1.07) ozone measurements derived from the infrared emission observations at 9.6 μm. The accuracy of the ozone measurements is of the order of 10% in the upper stratosphere-lower mesosphere region, with a positive bias increasing with altitude [*Rong et al*., 2009]. The vertical resolution of the observations is about 2 km [*Mlynczak*, 1997], and the latitudinal coverage changes with time, depending on the yaw period of the satellite, leading to the coverage changing from 83°S–52°N to 52°S–83°N every 60 days [*Rong et al*., 2009].

3. Definitions and Methods for Dynamics

[11] We use the World Meteorological Organization and *Charlton and Polvani* [2007] definition for sudden stratospheric warming events. The conditions for an SSW event are that (1) the zonal mean zonal wind is reversed (from westerly to easterly) at the 10 hPa level at 60°N and (2) the 10 hPa temperature gradient between 60°N and the pole becomes positive. If both conditions are fulfilled, the event is classified as a major SSW; otherwise, it is a minor SSW (e.g., when winds are reversed poleward of 60°N but not at 60°N). We used the operational zonal mean temperature and zonal mean zonal wind data from the European Centre for Medium-Range Weather Forecasts (ECMWF) and compared the 10 hPa zonal mean temperature/zonal wind at each latitude between 60°N and 90°N with the value at 60°N, 10 hPa. The results show that a major SSW took place on 23 January 2009 and that a strong minor warming took place on 14 January 2012.

[12] To characterize the dynamics in the polar regions even further and to examine the polar vortex conditions and mesosphere-to-stratosphere descent of air, we calculate the Northern Annular Mode (NAM) and CO Northern Annular Mode (CNAM) using EOF (empirical orthogonal function) analysis as described by *Baldwin and Dunkerton* [1999, 2001] and *Lee et al*. [2009, 2011]. The EOF analysis is carried out from MLS daily mean GPH and CO data for each altitude and on a 4° (latitude) × 8° (longitude) grid cell. The winter climatology over the 8 years of MLS measurements from 2005 to 2012 is then subtracted from the data, leaving GPH and CO anomalies. After area weighting the data, we computed the NAM and CNAM indices as the first EOF of the temporal covariance matrix (principal component). The NAM and CNAM indices are both normalized with the standard deviation of the indices. Details of applying EOF methods and further references can be found in *Baldwin and Dunkerton* [1999, 2001] and *Lee et al*. [2009, 2011].

4. Results

4.1. Middle Atmospheric Dynamics and EOF Analysis

[13] The NAM and CNAM indices for 2005, 2009, and 2012 in the NH are presented in Figure 2. In the figure, positive (red) NAM values are associated with a strong polar vortex and negative (blue) values with a weaker or displaced vortex. In all three years, the polar vortex either formed or was already formed in December and the NAM index shows a similar mesosphere-to-stratosphere progress of the vortex. While, in 2005, the vortex persisted until the end of February, in both 2009 and 2012, the vortex development was suddenly interrupted in late January (2009) and mid-January (2012). In addition, in late 2011 to early 2012, the NAM index turned negative in the upper stratosphere/lower mesosphere for a short period of time (~10 days), indicating a SSW event.

[14] An SSW took place also in both January 2009 and 2012, with slightly different timings. The effect of the SSWs can be seen from Figure 2 as an abrupt change of the NAM index from positive (strong polar vortex) to negative (vortex split/displacement) in both of these years. The changes after the SSWs in 2009 and 2012 are clear: The dynamics of the atmosphere were affected between about 10 and 95 km (2009) and between about 30 and 95 km (2012), with the effects of the 2009 SSW being more pronounced. In both cases, the polar vortex reformed at higher altitude after the stratospheric warming events and then progressed down to lower mesospheric and stratospheric altitudes. Regardless of the similarities in the upper mesospheric vortices after the SSW events in early 2009 and 2012, the polar vortex in the stratosphere before the SSWs was stronger

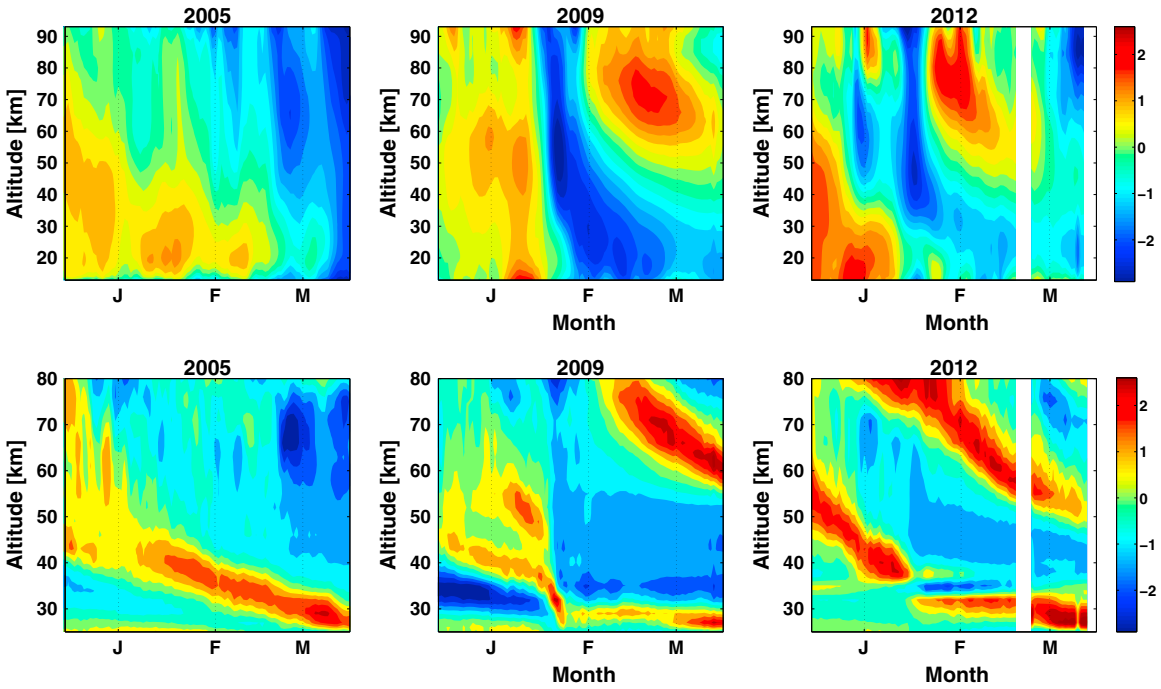

Figure 2. (top) NAM and (bottom) CNAM indices (see the text for more details) for 15 December to 15 March in 2005, 2009, and 2012 obtained from EOF analysis of the geopotential height and CO, respectively. Positive indices (red) represent conditions with a strong polar vortex (NAM) and a large amount of CO (CNAM), whereas negative indices (blue) represent conditions with a weak polar vortex (NAM) and only modest CO values (CNAM).

and more stable in 2012 than in 2009. In addition, the SSW in late 2011 to early 2012 affected the polar vortex at the mesospheric altitudes.

[15] The CNAM indices agree well with the NAM indices. The bottom panel of Figure 2 shows that there was mesosphere-to-stratosphere descent of CO in all three years. The rate of descent and the altitude range where the descent takes place appear to vary from year to year. During the 2004–2005 winter, the lower mesospheric air descended down to 25 km altitude with a descent rate of about 380 m/d which implies strong polar vortex conditions and low interference from atmospheric waves. In 2009 and 2012, SSWs took place in late January and mid-January, respectively, and interrupted the descent of the air. In both of these years, the descent continued, with increased descent rates, after the polar vortex reformed at a higher altitude following the warming events. By mid-March, the elevated CO values had descended to about 60 km (~570 m/d) and 50 km (~520 m/d) in 2009 and 2012, respectively.

4.2. Odd Nitrogen

[16] Figure 3 shows ACE-FTS observations of both daily mean NO_x (ppbv) and the change in NO_x (%) relative to the January–March mean in 2007–2008 in early 2005, 2009, and 2012 poleward from 60°N. The white dashed lines indicate the onset of SPEs, while the red solid lines indicate the onset of SSWs. The SPEs took place on 16 January 2005, 23 and 28 January 2012, and 7 and 13 March 2012.

[17] In 2005, the SPE (the proton fluxes have been described by *Seppälä et al.* [2006]) significantly affects NO_x volume mixing ratios between 45 and 80 km [see also *Jackman et al.*, 2011]. The ACE-FTS observations (Figure 3b, top) show 30–300% increases in NO_x right after the onset of the event. Because of the strong polar vortex in the stratosphere, NO_x was transported downward from early January, and elevated amounts (~10–20 ppbv) can be seen above about 45 km before the SPE onset (Figure 3a, top). The stratospheric vortex started to weaken in mid-February, reducing the levels of the SPE-produced NO_x in the stratosphere. Strong descent of mesospheric NO_x did not take place since; unlike in the stratosphere, the vortex was weak at higher altitudes (Figure 2) during the whole of early 2005.

[18] The major SSW in late January 2009 (23 January) and the following reformation of the stratopause at about 80 km altitude led to formation of a strong polar vortex that persisted until mid-March (Figure 2). The ACE-FTS observations (Figure 3a, middle) show NO_x descending inside the vortex from mesospheric altitudes down to about 50 km with mixing ratios of 20–300 ppbv, i.e., a factor of 10–25 higher than before the descent. The descent stops when the final vortex split takes place, just before the maximum of the NO_x descent feature reaches the stratosphere. This can also be seen in Figure 4, which presents the NO_x column densities around the stratopause during the different winters. The mesospheric NO_x enhancement is likely a result of the strong downwelling since no SPEs providing in situ production occurred. The overall geomagnetic activity was rather low in early 2009, which suggests that significant in situ production of NO_x by electron precipitation was also unlikely [*Randall et al.*, 2009]. Discontinuity in the data, i.e., lower abundances of NO_x (Figure 3a, middle) and decrease in NO_x (Figure 3b, middle), in the middle of the strong descent around mid-

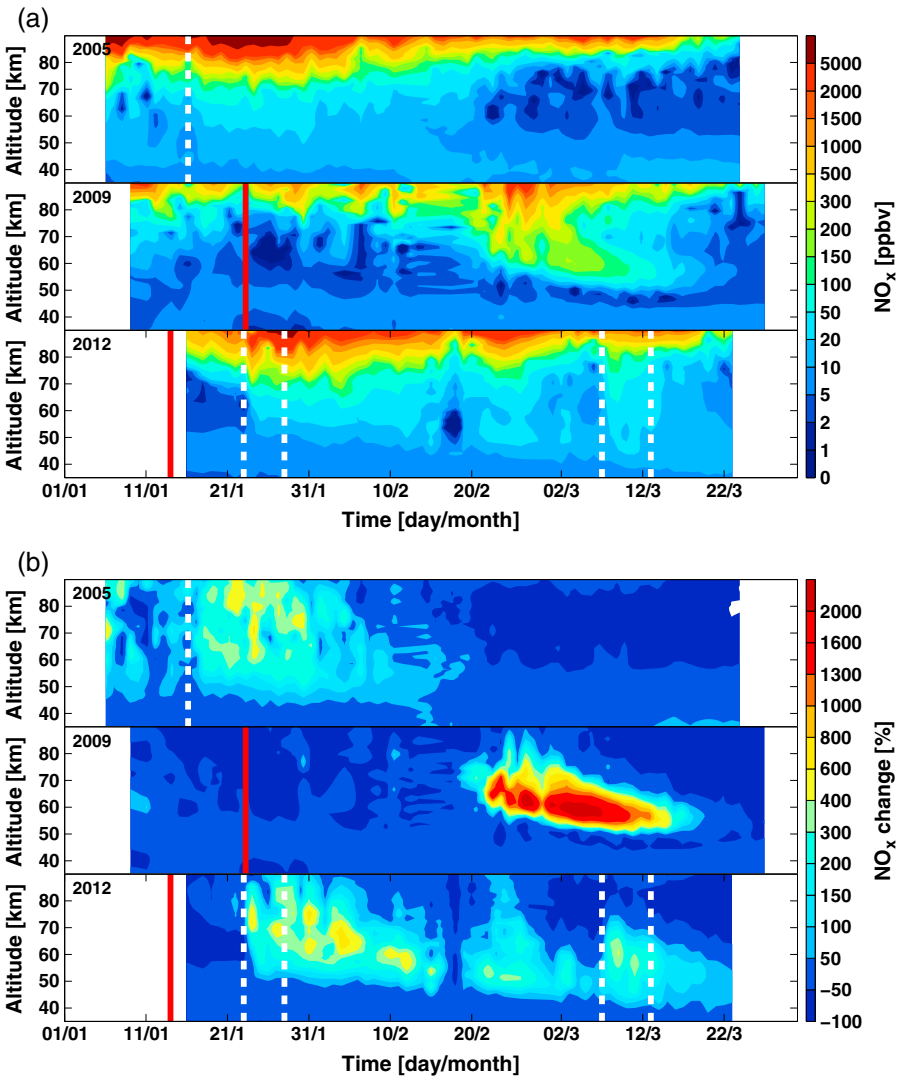

Figure 3. (a) NO_x mixing ratio (ppbv) and (b) change in NO_x (%) relative to the January–March mean in 2007–2008 calculated from ACE-FTS observations. For all figures, the observations shown are northward of 60°N in early 2005 ((a) and (b) top panels), 2009 (middle panels), and 2012 (bottom panels). The white dashed lines indicate the time points of the observed SPEs and the red solid lines the observed SSWs during these years.

February is due to the limited latitudinal coverage of the instrument (Figure 1): At this time, ACE-FTS was measuring at lower latitudes where the solar illumination and polar vortex conditions are already different to those farther in north. A similar effect is seen also in early February to mid-February 2012 (Figures 3a, bottom, and 3b, bottom).

[19] In 2012, a strong minor SSW took place in mid-January (14 January), i.e., earlier than the major SSW in 2009, and the CNAM indices (Figure 2) show descent of mesospheric air down to about 45 km by the end of March. A similar descent is seen in the ACE-FTS NO_x observations (Figures 3a, bottom, and 3b, bottom): Elevated amounts of NO_x reach altitudes of even 40 km by mid-March. Compared to the descent in 2009, the descent rates in 2012 were moderate (see section 4.1). However, lower altitudes were affected because the SSW, which started the descent event, occurred earlier than in 2009. In addition to the favorable dynamical conditions aiding the NO_x descent, there were several SPEs in early 2012, enabling in situ production of NO_x in the mesosphere and upper stratosphere. First, two SPEs took place in January (starting on 23 and 27 January). The >10 MeV proton fluxes, which will impact altitudes of about 70 km and below [*Turunen et al.*, 2009],were elevated for 9 days from the start of the first event, before returning to pre-SPE levels. It should be noted that the proton precipitation levels at lower energies were, in fact, elevated before the SPE, from 20 January. The peak >10 MeV proton flux was measured at 6310 pfu (particle flux unit, particles $cm^{-2}\,s^{-1}\,sr^{-1}$), making the event comparable with the January 2005 event (pfu of 5040; see *Seppälä et al.* [2006]). Another two SPEs took place in March (7 and 13 March), again with elevated precipitation starting earlier (5 March). The March events were comparable with the January events with a peak >10 MeV proton flux measured at 6530 pfu and a total duration from the start of the first SPE to return to pre-SPE levels taking 9 days.

[20] The ACE-FTS observations show NO_x descent already a couple of days after the SSW and a sudden, up to

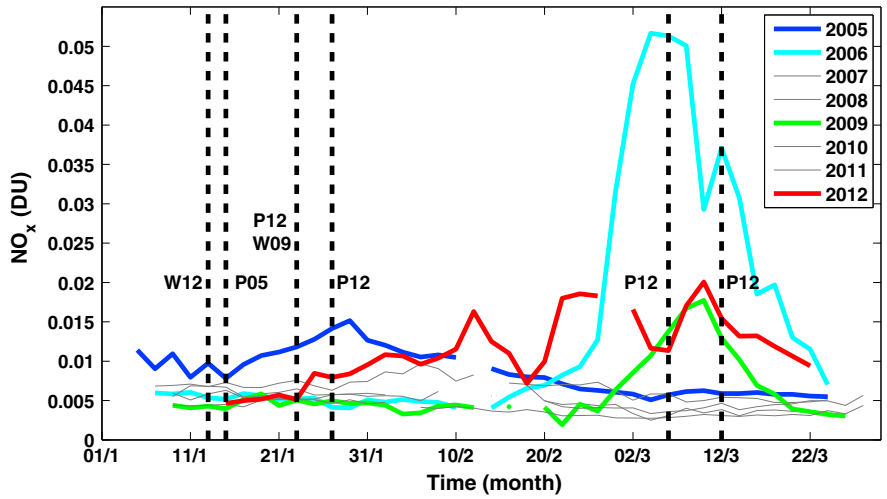

Figure 4. Two day mean NO_x column (DU) for altitude range 46–56 km calculated from ACE-FTS observations for the polar cap region (60°N–90°N). The dashed lines show the time points for SPEs (P) and SSWs (W) during 2005 (05), 2009 (09), and 2012 (12).

800% increase in NO_x mixing ratios above altitudes of about 50 km, with a 50–100% increase below 50 km, right after the first SPE (Figure 3b, bottom). The second proton event in late January seemed to have less of an effect on the already elevated NO_x levels. The first SPE in March, on the other hand, increased the amount of NO_x rapidly from 80 km down to even 40 km with a magnitude comparable to the first event in January, whereas the final SPE in mid-March caused an increase of 50–100% mainly between 40 and 45 km.

[21] Figure 4 compares the overall effects of particle precipitation activity and atmospheric dynamical processes on NO_x (Dobson unit, DU) around the stratopause between 46 and 56 km for years 2005–2012. The dashed lines show the onset times for SPEs and SSWs in 2005, 2009, and 2012. The figure shows that the amount of NO_x in the middle atmosphere in March is higher (>0.005 DU) during years with SSW events (2006, 2009, and 2012) than in dynamically nonactive years. These SSWs took place around January, but the effect on NO_x at stratopause altitudes is seen with a delay. This demonstrates the time needed for NO_x to descend from mesospheric altitudes down to the stratosphere inside the polar vortex. On the other hand, the NO_x increments due to SPEs are visible immediately after the events in January 2005 and January and March 2012. The changes in NO_x after these

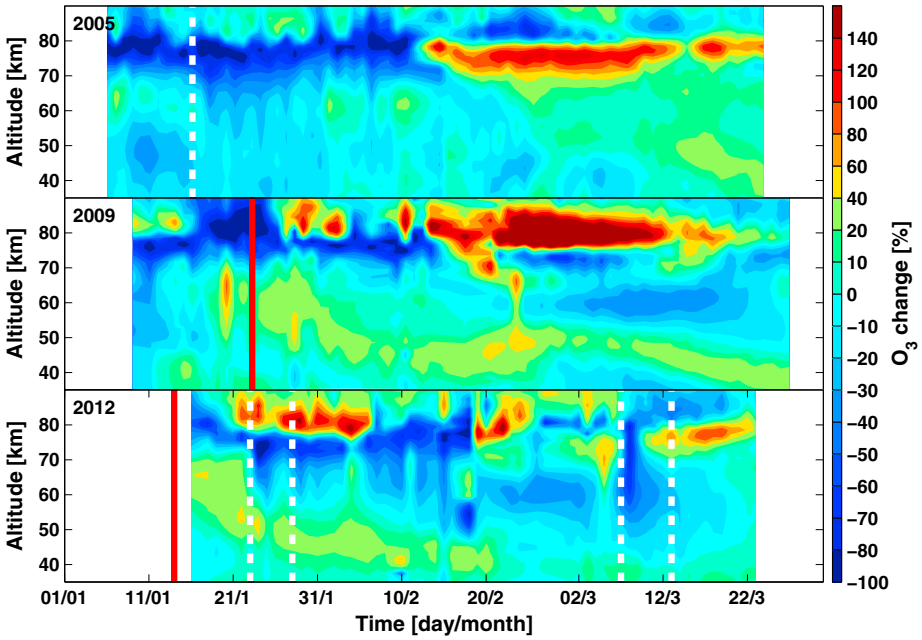

Figure 5. ACE-FTS observations of the change in O_3 (%) relative to the January–March mean in 2007–2008 northward of 60°N in (top) 2005, (middle) 2009, and (bottom) 2012. The white dashed lines indicate the time points of the observed SPEs and the red solid lines the observed SSWs during these years.

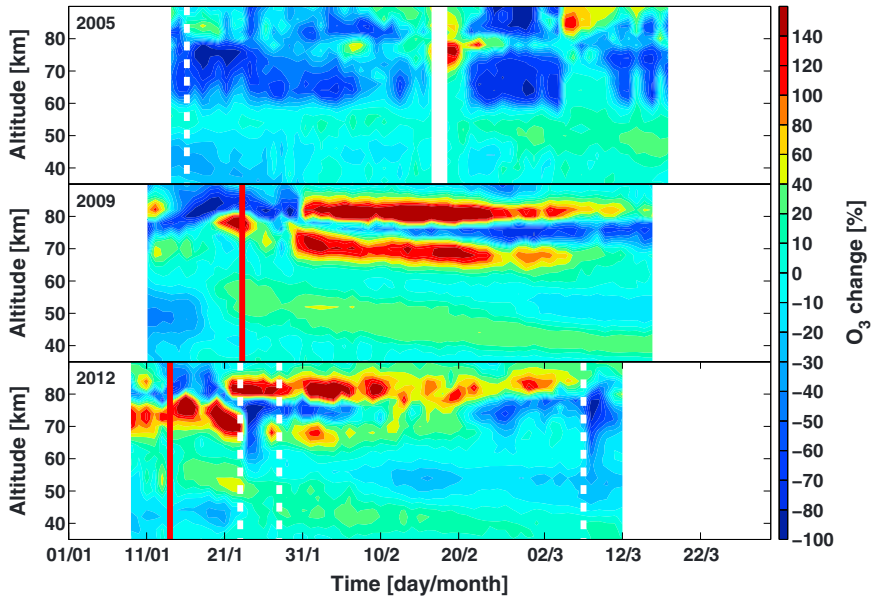

Figure 6. SABER observations of the change in O_3 (%) relative to the January–March mean in 2007–2008 between 65°N and 75°N in (top) 2005, (middle) 2009, and (bottom) 2012. Also, the observed SPEs (white dashed lines) and SSWs (red solid lines) are marked in the figure.

events last for varying periods of time (from couple to few days), also depending on atmospheric dynamics and the solar illumination conditions at the altitudes in question during these years. It is interesting to note that the largest NO_x amounts at the typical stratopause altitudes are observed in March 2006. This is observed despite the overall NO_x enhancements being larger during 2009 [see *Randall et al.*, 2009]. Like in 2009, as discussed earlier, the descent in 2006 stops before the maximum of the descending NO_x feature reaches ~50 km altitudes, limiting the main impact to mesospheric altitudes.

4.3. Ozone

[22] Ozone observations, which were available from ACE-FTS, SABER, and MLS, are shown in Figures 5–7, respectively. All three satellite instruments observe the NH polar cap region but use different techniques and have slightly different coverages. ACE-FTS only covers a narrow latitude band and is moving toward the south around mid-February and then returning back to higher latitudes (Figure 1), whereas both MLS and SABER observe all the latitudes except the very pole (here we use the latitude band

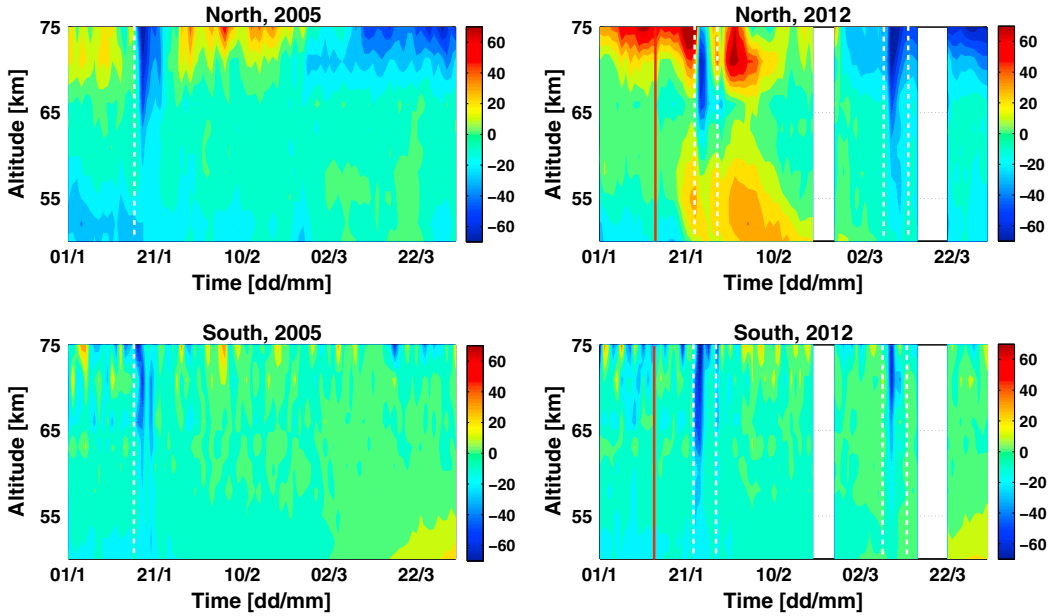

Figure 7. MLS observations of the change in nighttime O_3 at mesospheric altitudes for geomagnetic latitudes 65°N–75°N (top) and 65°S–75°S (bottom). The percent change is calculated relative to the January–March mean in 2007–2008. The white dashed lines indicate the observed SPEs and the red solid lines the SSW in 2012. Contour lines are shown in 10% steps between −70% and 70%.

Table 1. Changes in Ozone (%) After Solar Proton Events in January 2005 and in Early 2012 Relative to the January–March Mean in 2007–2008[a]

	ACE-FTS	MLS	SABER
	% (km)	% (km)	% (km)
2005	20–70 (45–80)	20–70 (50–80)	20–90 (55–80)
2012 (I)	10–80 (55–75)	10–70 (55–80)	10–90 (50–80)
2012 (II)	10–60 (55–75)	10–70 (63–80)	20–70 (70–80)
2012 (III)	10–70 (40–90)	10–70 (45–80)	20–90 (45–85)
2012 (IV)	20–30 (40–70)		

[a]The four cases for 2012 indicate the different SPEs that took place in January (I and II) and March (III and IV). In brackets is given the altitude range (in km) where the changes were observed. Empty fields stand for no available data.

65°N–75°N). Therefore, the results from the different instruments can reflect differences due to, e.g., different solar illumination and polar vortex conditions in the measurement locations. In addition, the instruments measure ozone with differing vertical resolutions as discussed earlier: The resolution is about 4 km for ACE-FTS, 2–3 km below 65 km and 5 km above for MLS, and about 2 km for SABER. It is important to note that this may affect how some features in the vertical profiles are seen by the different instruments. Because we use the MLS observations also to look at hemispheric differences in response to the SPEs, the MLS values are calculated for geomagnetic latitudes to ensure that a maximum amount of data is within the area where energetic particles precipitate. We also checked the results for geographic latitude, and the use of geomagnetic latitudes did not change the results significantly.

[23] The SPE-related ozone changes for 2005 and 2012, as seen in Figures 5–7, are summarized in Table 1. The changes are calculated relative to the January–March mean in 2007–2008 (no SSWs or SPEs) separately for every instrument. To help separate the individual 2012 SPEs, the results in Table 1 are given separately for the four SPEs in January and March 2012 and are labeled as I–IV according to their order of occurrence. The three satellite instruments all show reductions in ozone levels after the SPEs in 2005 and 2012. The depletion is restricted mainly to the altitude range of 50–80 km for 2005 and 40–80 km for 2012. The decreases are from about 20% up to 80% in 2005 and 10–90% in 2012. The reduction in ozone lasted longer in 2012 when a number of SPEs and a strong minor SSW occurred (in 2005, there was only one SPE): from late January to late March. While the short-term (few days) ozone losses observed directly after the SPEs are driven by chemical loss from enhanced SPE-produced HO_x [*Verronen et al.*, 2006], the observed longer-term depletion in lower mesospheric/upper stratospheric ozone in 2009 and especially in 2012 is more complex. In 2009, with only a major SSW affecting the middle atmosphere, the observations show (Figures 5 and 6) a decrease of 10–40% in ozone between about 45 and 75 km, coinciding with the NO_x descent maximum (Figure 3).

[24] For comparison of the SPE effects, we included MLS measurements also from the Southern Hemisphere (SH) summer in Figure 7. The January to March period in the south is summer/autumn season, i.e., non-polar-vortex conditions. The effect seen in ozone is thus only due to the SPE-driven chemical effects. The observations show that after the SPE in early 2005 (left), the amount of ozone decreases by 10–70% between 55 and 80 km. In 2012 (right), ozone decreases by 10–60% between 60 and 80 km (events I and III) and by 10–30% between 60 and 70 km (event II). For event IV, no MLS data were available. The magnitude of the ozone losses in the SH is comparable to those of the NH, but the NH changes last longer, due to lack of solar radiation and stable conditions inside the NH polar vortex at that time of the year, which prevent effective NO_x destruction.

5. Discussion

[25] In early 2012, when both a descent event of NO_x following a SSW in mid-January and in situ production of NO_x due to several SPEs during the period of January–March took place, both short-term and long-term ozone changes were observed. The SPE-related short-term (few days) ozone losses in early 2012 are driven by the enhanced HO_x, the main chemical catalyst of ozone loss in the mesosphere [e.g., *Grenfell et al.*, 2006].

[26] Understanding the longer-term (weeks) ozone depletion in the mesosphere and upper stratosphere is less straightforward. Figure 8 shows the changes in ozone in 2004–2012 relative to the 2007–2008 January–March mean from the ACE-FTS observations. The overlaid contours show the positive changes in NO_x (relative to the same period). It is clear that during years with enhanced NO_x in the middle atmosphere, e.g., in 2004 and 2012, also decreases in ozone are observed. In the mesosphere, the reaction rates of the NO_x catalytic cycles depleting ozone are dominated by those of the HO_x cycles, leading to the HO_x-driven ozone loss at those altitudes as discussed above. Closer to the stratopause region, and below, the catalytic NO_x cycles become comparable to the catalytic HO_x and chlorine cycles, becoming increasingly important to the chemical ozone balance.

[27] Changes in dynamics following SSW events are also likely contributing to the observed long-term ozone loss. *Sofieva et al.* [2012] suggested that during SSW events, the upper stratospheric and mesospheric ozone is affected by the negative temperature-ozone correlation and transport of ozone-poor air masses from higher altitudes. The ozone loss cycles could also be affected by the SSW-driven changes in temperatures, such as those reported by *Randall et al.* [2009]. It is also important to note that SSW events create a possibility for subtropical air to be transported to polar latitudes, further complicating the dynamical ozone balance in polar stratospheric air masses [*Konopka et al.*, 2007]. Due to the complexity of the situation, it is not possible to separate all these processes contributing to the ozone balance from observations alone to assess their relative importance. The detailed analysis of the different chemical and dynamical components requires the use of a chemistry transport model. This is, however, out of the scope of this paper and will be the topic of a further study focusing on the modeling aspect.

[28] Apart from ozone losses, the observations also indicate increases in ozone. In 2009 and 2012, ozone increases in the stratosphere are seen after the SSWs starting from above 50 km and descending down to ~40 km. These changes can be understood by polar vortex dynamics: When the vortex weakens, ozone-rich air from lower latitudes is mixed with the ozone-poor air inside the vortex, leading to the observed increases in ozone. This process can be clearly seen through the trace gases, such as CO and water vapor, which

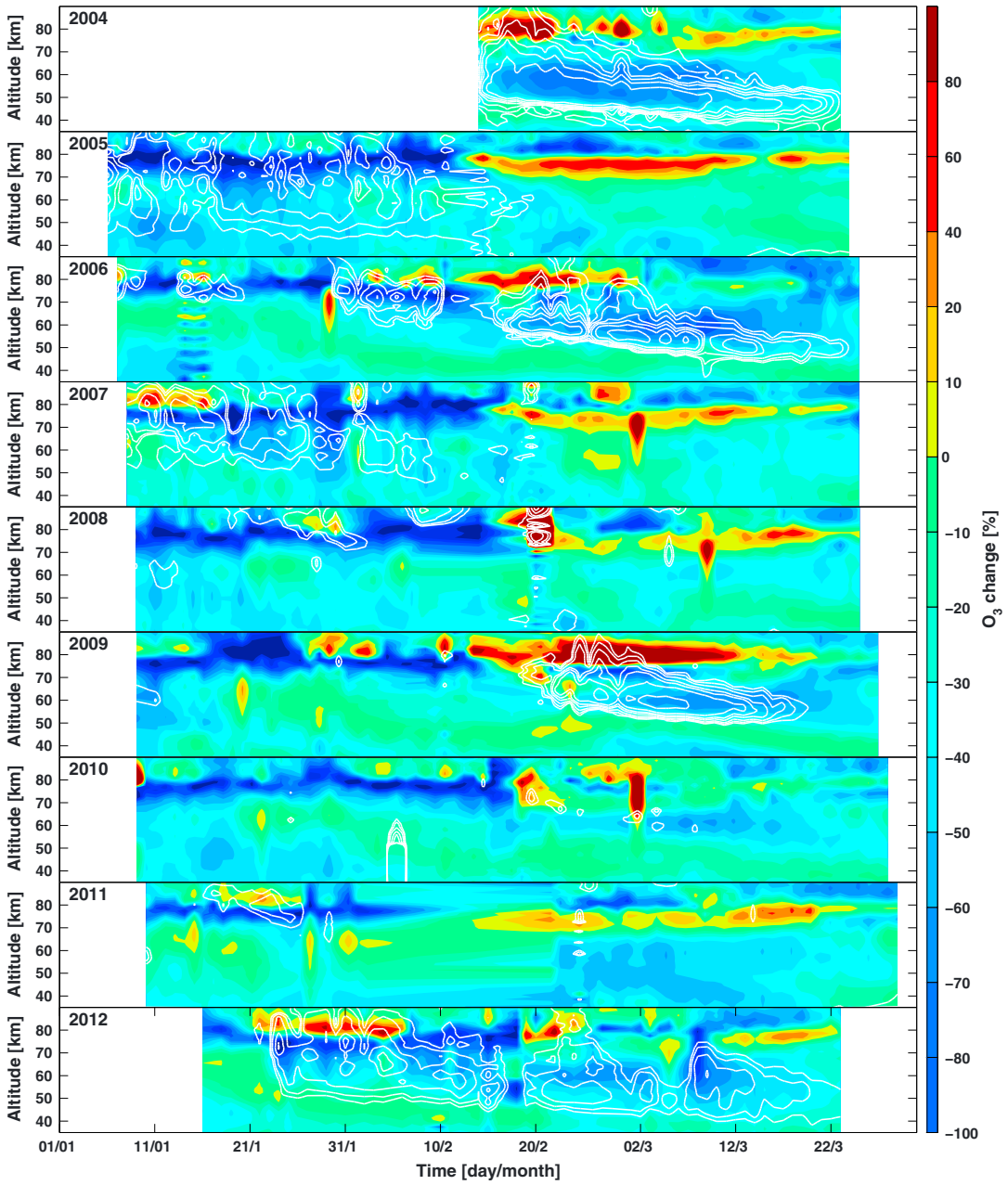

Figure 8. ACE-FTS observations of the change in O_3 (%) relative to the January–March mean in 2007–2008 northward of 60°N in 2004–2012. The overlaid contours are values of positive NO_x changes relative to the same period (50, 100, 200, 400, 600, 1000, and 2000%).

are mixed out of the vortex after SSW and transported into a strong reformed upper stratospheric/lower mesospheric vortex (as discussed by *Manney et al.* [2009] for the 2009 case). Higher up, in the MLT region, both the downward transport of the HO_x layer from the same altitude region and the descent of upper atmospheric air with high amounts of atomic oxygen increasing ozone production contribute to the increases [*Smith et al.*, 2009; *Damiani et al.*, 2010; *Sofieva et al.*, 2012]. In all cases, other effects, due to, e.g., the final warming timing and seasonal changes, need to be taken into account for a complete picture.

[29] Previous studies have shown a correlation between geomagnetic activity and the amount of NO_x in the NH stratosphere [e.g., *Seppälä et al.*, 2007; *Arnone and Hauchecorne*, 2012, and references therein]. Significant ozone losses following stratospheric NO_x enhancements have been reported on two different types of occasions: (1) following very large SPEs such as the Halloween event in 2003 [see, e.g., *Seppälä et al.*, 2004; *Jackman et al.*, 2009; *Funke et al.*, 2011] and (2) strong downward descent events following SSW, with existing NO_x enhancements from energetic particle precipitation such as the descent event in early 2004 [*López-Puertas et al.*, 2005; *Randall et al.*, 2005; *Clilverd et al.*, 2009]. Our results show that although the SPEs in 2005 and 2012 increased the amounts of NO_x in the mesosphere and upper stratosphere, the in situ production

was not sufficient enough to have a clearly NO_x-dominated effect on the middle atmospheric ozone. Similar results for mesospheric altitudes for the 2012 SPEs have now also been shown by *von Clarmann et al*. [2013] using a different satellite instrument than our study. The MIPAS observations reported by *von Clarmann et al*. [2013] suggest similar NO_x enhancements for the first three SPEs in 2012 as the ACE-FTS, MLS, and SABER observations we analyzed, but following the final SPE in mid-March, MIPAS shows lower increases (about 2–5 ppbv). *von Clarmann et al*. [2013] also report ozone losses coinciding with the NO_x enhancements at mesospheric altitudes following the January SPEs.

[30] It is important to note here that these SPEs were small to medium in strength, and much larger events have been observed in the past (including the 2003 SPEs). In fact, in January–February 2012, the monthly mean geomagnetic A_p index (available from the Space Physics Interactive Data Resource, http://spidr.ngdc.noaa.gov), used as a proxy for overall particle precipitation levels, was much lower (~7–9) than that at the same time in 2004 (~13–22) when enhanced amounts of NO_x due to energetic particle precipitation were transported to the stratosphere, and clear ozone losses were observed. For 2012, this means that the overall MLT NO_x production by energetic particle precipitation was very low. Consequently, any mesospheric air masses transported to the stratosphere would have relatively low concentrations of NO_x. Similar conditions low overall particle precipitation levels and, additionally, no SPEs for MLT NO_x production took place in 2009. Nevertheless, mesospheric production of NO_x can have an important role in intensifying the MLT NO_x-stratospheric ozone connection since the downward transport of thermosphere air masses through the mesopause is hindered by the upper atmosphere circulation patterns, and the transport from the lower thermosphere to the mesosphere arises mainly from diffusion processes [*Smith et al*., 2011].

[31] If the determining factor indeed is the level of NO_x production from the prevailing energetic particle precipitation, including SPEs, it is likely that the NO_x-ozone connection is more pronounced during and after solar maximum periods (2003–2004) than during and after solar minimum periods (the 2009 and 2012 events). Therefore, our results, which, for the strong descent event part, represent an exceptionally quiet solar minimum period, should not be used to draw conclusions for all situations but rather for conditions where the overall energetic particle precipitation levels influencing NO_x in the MLT were below average.

6. Conclusions

[32] The aim of this study was to compare years with SPEs and/or SSWs and the effects of different combinations of these events on middle atmospheric NO_x and ozone. The results show that the amount of NO_x increased due to both the SPEs (2005 and 2012) and SSWs (2009 and 2012) by a factor of 1 to 25 between 40 and 90 km depending on the year and event. Ozone losses, both short term and long term, of the order of 10–90% between 40 and 90 km were also observed. Comparing the three years, the largest mesospheric NO_x changes were observed in 2009 following the major SSW in late January. In 2012, when both SPEs and a SSW took place, enhanced amounts of NO_x were transported down to 40 km altitude, i.e., lower than in years 2005 and 2009. As a result, the largest NO_x changes in the upper stratosphere were seen in 2012.

[33] Our main result is that the combination of optimal dynamics, i.e., downward transport following a mid-January SSW, and in situ production of NO_x due to several moderate SPEs is not necessarily enough to produce a long-term and clearly NO_x-dominated effect on stratospheric ozone. Particularly in the case of 2012, (1) the SPEs were only medium size in strength and did not produce enough NO_x and (2) the overall production of NO_x by particle precipitation in the MLT region was low, leading to relatively low concentrations of NO_x being transported down to the stratosphere after the SSW. It should be noted that the cases presented in this paper are from an elongated period of relatively low solar activity. In order to fully understand the NO_x connection between the MLT and stratosphere and its influence on stratospheric ozone levels, periods of high solar activity (for high overall energetic particle precipitation) should be investigated as well. For this, the continuation of middle atmosphere measurements of NO_x and ozone is essential.

[34] **Acknowledgments.** The work of S.-M.P. was supported by the Academy of Finland through project 134325 (MIDAT: Middle atmosphere dynamics and chemistry in climate change), the work of A.S. was supported by the Academy of Finland through projects 258165 and 265005 (CLASP: Climate and Solar Particle Forcing), and the works of M.E.A. and P.T.V. were supported by the Academy of Finland through projects 136225 and 140888 (SPOC: Significance of Energetic Electron Precipitation to Odd Hydrogen, Ozone, and Climate). The Atmospheric Chemistry Experiment (ACE), also known as SCISAT, is a Canadian-led mission mainly supported by the Canadian Space Agency and the Natural Sciences and Engineering Research Council of Canada. We are grateful to NASA for providing the MLS Aura data and the SABER team for providing the SABER data.

References

Arnone, E., and A. Hauchecorne (2012), Stratosphere NO_y species measured by MIPAS and GOMOS onboard ENVISAT during 2002–2010: Influence of plasma processes onto the observed distribution and variability, *Space Sci. Rev.*, *168*, 315–332, doi:10.1007/s11214-011-9861-1.

Baldwin, M. P., and T. J. Dunkerton (1999), Downward propagation of the Arctic oscillation from the stratosphere to the troposphere, *J. Geophys. Res.*, *104*, 30,937–30,946, doi:10.1029/1999JD900445.

Baldwin, M. P., and T. J. Dunkerton (2001), Stratospheric harbingers of anomalous weather regimes, *Science*, *294*, 581–584, doi:10.1126/science.1063315.

Barth, C. A. (1992), Nitric oxide in the lower thermosphere, *Planet. Space Sci.*, *40*, 315–336.

Baumgaertner, A. J. G., A. Seppälä, P. Jöckel, and M. A. Clilverd (2011), Geomagnetic activity related NO_x enhancements and polar surface air temperature variability in a chemistry climate model: Modulation of the NAM index, *Atmos. Chem. Phys.*, *11*, 4521–4531, doi:10.5194/acp-11-4521-2011.

Bernath, P. F., et al. (2005), Atmospheric Chemistry Experiment (ACE): Mission overview, *Geophys. Res. Lett.*, *32*, L15S01, doi:10.1029/2005GL022386.

Callis, L. (1997), Odd nitrogen formed by energetic electron precipitation as calculated from TIROS data, *Geophys. Res. Lett.*, *24*, 3237–3240, doi:10.1029/97GL03276.

Callis, L. B., and J. D. Lambeth (1998), NO_y formed by precipitating electron events in 1991 and 1992: Descent into the stratosphere as observed by ISAMS, *Geophys. Res. Lett.*, *25*, 1875–1878, doi:10.1029/98GL01219.

Callis, L. B., D. N. Baker, J. B. Blake, J. D. Lambeth, R. E. Boughner, M. Natarajan, R. W. Klebesadel, and D. J. Gorney (1991a), Precipitating relativistic electrons: Their long-term effect on stratospheric odd nitrogen levels, *J. Geophys. Res.*, *96*, 2939–2976.

Callis, L. B., R. E. Boughner, M. Natarajan, J. D. Lambeth, D. N. Baker, and J. B. Blake (1991b), Ozone depletion in the high latitude lower stratosphere: 1979–1990, *J. Geophys. Res.*, *96*, 2921–2937.

Callis, L. B., et al. (1996a), Precipitation electrons: Evidence for effects on mesospheric odd nitrogen, *Geophys. Res. Lett.*, *23*, 1901–1904, doi:10.1029/96GL01787.

Callis, L. B., D. N. Baker, M. Natarajan, J. B. Blake, R. A. Mewaldt, R. S. Selesnick, and J. R. Cummings (1996b), A 2-D model simulation of downward transport of NO_y into the stratosphere: Effects on the 1994 austral spring O_3 and NO_y, *Geophys. Res. Lett.*, *23*, 1905–1908, doi:10.1029/96GL01788.

Charlton, A. J., and L. M. Polvani (2007), A new look at stratospheric sudden warmings. Part I: Climatology and modeling benchmarks, *J. Clim.*, *20*, 449–469, doi:10.1175/JCLI3996.1.

Clilverd, M. A., A. Seppälä, C. J. Rodger, P. T. Verronen, and N. R. Thomson (2006), Ionospheric evidence of thermosphere-to-stratosphere descent of polar NO_x, *Geophys. Res. Lett.*, *33*, L19811, doi:10.1029/2006GL026727.

Clilverd, M. A., A. Seppälä, C. J. Rodger, M. G. Mlynczak, and J. U. Kozyra (2009), Additional stratospheric NO_x production by relativistic electron precipitation during the 2004 spring NO_x descent event, *J. Geophys. Res.*, *114*, A04305, doi:10.1029/2008JA013472.

Damiani, A., M. Storini, M. L. Santee, and S. Wang (2010), Variability of the nighttime OH layer and mesospheric ozone at high latitudes during northern winter: Influence of meteorology, *Atmos. Chem. Phys.*, *10*, 14,583–14,610, doi:10.5194/acpd-10-14583-2010.

Funke, B., M. López-Puertas, S. Gil-Lopez, T. von Clarmann, G. P. Stiller, H. Fischer, and S. Kellmann (2005), Downward transport of upper atmospheric NOx into the polar stratosphere and lower mesosphere during the Antarctic 2003 and Arctic 2002/2003 winters, *J. Geophys. Res.*, *110*, D24308, doi:10.1029/2005JD006463.

Funke, B., M. López-Puertas, H. Fischer, G. P. Stiller, T. von Clarmann, G. Wetzel, B. Carli, and C. Belotti (2007), Comment on "Origin of the January–April 2004 increase in stratospheric NO_2 observed in northern polar latitudes" by Jean-Baptiste Renard et al., *Geophys. Res. Lett.*, *34*, L07813, doi:10.1029/2006GL027518.

Funke, B., et al. (2011), Composition changes after the "Halloween" solar proton event: The High-Energy Particle Precipitation in the Atmosphere (HEPPA) model versus MIPAS data intercomparison study, *Atmos. Chem. Phys.*, *11*, 9089–9139, doi:10.5194/acp-11-9089-2011.

Grenfell, J. L., R. Lehmann, P. Mieth, U. Langematz, and B. Steil (2006), Chemical reaction pathways affecting stratospheric and mesospheric ozone, *J. Geophys. Res.*, *111*, D17311, doi:10.1029/2004JD005713.

Hauchecorne, A., J.-L. Bertaux, F. Dalaudier, J. M. Russell, M. G. Mlynczak, E. Kyrölä, and D. Fussen (2007), Large increase of NO_2 in the north polar mesosphere in January–February 2004: Evidence of a dynamical origin from GOMOS/ENVISAT and SABER/TIMED data, *Geophys. Res. Lett.*, *34*, L03810, doi:10.1029/2006GL027628.

Jackman, C. H., E. L. Fleming, and F. M. Vitt (2000), Influence of extremely large solar proton events in a changing stratosphere, *J. Geophys. Res.*, *105*, 11,659–11,670.

Jackman, C. H., et al. (2008), Short- and medium-term atmospheric constituent effects of very large solar proton events, *Atmos. Chem. Phys.*, *8*, 765–785, doi:10.5194/acp-8-765-2008.

Jackman, C. H., D. R. Marsh, F. M. Vitt, R. R. Garcia, C. E. Randall, E. L. Fleming, and S. M. Frith (2009), Long-term middle atmospheric influence of very large solar proton events, *J. Geophys. Res.*, *114*, D11304, doi:10.1029/2008JD011415.

Jackman, C. H., et al. (2011), Northern Hemisphere atmospheric influence of the solar proton events and ground level enhancement in January 2005, *Atmos. Chem. Phys.*, *11*, 6153–6166, doi:10.5194/acp-11-6153-2011.

Jiang, Y. B., et al. (2007), Validation of Aura Microwave Limb Sounder ozone by ozonesonde and lidar measurements, *J. Geophys. Res.*, *112*, D24S34, doi:10.1029/2007JD008776.

Konopka, P., et al. (2007), Ozone loss driven by nitrogen oxides and triggered by stratospheric warmings can outweigh the effect of halogens, *J. Geophys. Res.*, *112*, D05105, doi:10.1029/2006JD007064.

Lee, J. N., D. L. Wu, G. L. Manney, and M. J. Schwartz (2009), Aura Microwave Limb Sounder observations of the Northern Annular Mode: From the mesosphere to the upper troposphere, *J. Geophys. Res.*, *36*, L20807, doi:10.1029/2009GL040678.

Lee, J. N., D. L. Wu, G. L. Manney, M. J. Schwartz, A. Lambert, N. J. Livesey, K. R. Minschwaner, H. C. Pumphrey, and W. G. Read (2011), Aura Microwave Limb Sounder observations of the polar middle atmosphere: Dynamics and transport of CO and H_2O, *J. Geophys. Res.*, *116*, D05110, doi:10.1029/2010JD014608.

Livesey, N. J., et al. (2011), EOS MLS Version 3.3 Level 2 data quality and description document, Rep. JPL D-33509, Jet Propul. Lab., Pasadena, Calif.

López-Puertas, M., B. Funke, S. Gil-López, T. von Clarmann, G. P. Stiller, M. Höpfner, S. Kellmann, H. Fischer, and C. H. Jackman (2005), Observation of NO_x enhancement and ozone depletion in the Northern and Southern Hemispheres after the October–November 2003 solar proton events, *J. Geophys. Res.*, *110*, A09S43, doi:10.1029/2005JA011050.

Manney, G. L., M. J. Schwartz, K. Krüger, M. L. Santee, S. Pawson, J. N. Lee, W. H. Daffer, R. A. Fuller, and N. J. Livesey (2009), Aura Microwave Limb Sounder observations of dynamics and transport during the record-breaking 2009 Arctic stratospheric major warming, *Geophys. Res. Lett.*, *36*, L12815, doi:10.1029/2009GL038586.

Matsuno, T. (1971), A dynamical model of the sudden stratospheric warming, *J. Atmos. Sci.*, *28*, 1479–1494.

Mlynczak, M. G. (1997), Energetics of the mesosphere and lower thermosphere and the SABER experiment, *Adv. Space Res.*, *20*, 1177–1183.

Mlynczak, M. G., et al. (2005), Energy transport in the thermosphere during the solar storms of April 2002, *J. Geophys. Res.*, *110*, A12S25, doi:10.1029/2005JA011141.

Pumphrey, H. C., et al. (2007), Validation of middle-atmosphere carbon monoxide retrievals from the Microwave Limb Sounder on Aura, *J. Geophys. Res.*, *112*, D24S38, doi:10.1029/2007JD008723.

Randall, C. E., et al. (2005), Stratospheric effects of energetic particle precipitation in 2003–2004, *Geophys. Res. Lett.*, *32*, L05802, doi:10.1029/2004GL022003.

Randall, C. E., V. L. Harvey, C. S. Singleton, P. F. Bernath, C. D. Boone, and J. U. Kozyra (2006), Enhanced NO_x in 2006 linked to upper stratospheric Arctic vortex, *Geophys. Res. Lett.*, *33*, L18811, doi:10.1029/2006GL027160.

Randall, C. E., V. L. Harvey, D. E. Siskind, J. France, P. F. Bernath, C. D. Boone, and K. A. Walker (2009), NO_x descent in the Arctic middle atmosphere in early 2009, *Geophys. Res. Lett.*, *36*, L18811, doi:10.1029/2009GL039706.

Rong, P. P., J. M. Russell, M. G. Mlynczak, E. E. Remsberg, B. T. Marshall, L. L. Gordley, and M. López-Puertas (2009), Validation of Thermosphere Ionosphere Mesosphere Energetics and Dynamics/Sounding of the Atmosphere using Broadband Emission Radiometry (TIMED/SABER) v1.07 ozone at 9.6 μm in altitude range 15–70 km, *J. Geophys. Res.*, *114*, D04306, doi:10.1029/2008JD010073.

Russell, J. M., III, M. G. Mlynczak, L. L. Gordley, J. Tansock, and R. Esplin (1999), An overview of the SABER experiment and preliminary calibration result, *Proc. Soc. Photo. Opt. Instrum. Eng.*, *3756*, 277–288.

Salmi, S.-M., P. T. Verronen, L. Thölix, E. Kyrölä, L. Backman, A. Y. Karpechko, and A. Seppälä (2011), Mesosphere-to-stratosphere descent of odd nitrogen in February–March 2009 after sudden stratospheric warming, *Atmos. Chem. Phys.*, *11*, 4645–4655, doi:10.5194/acp-11-4645-2011.

Schwartz, M. J., et al. (2008), Validation of the Aura Microwave Limb Sounder temperature and geopotential height measurements, *J. Geophys. Res.*, *113*, D15S11, doi:10.1029/2007JD008783.

Semeniuk, K., J. C. McConnell, and C. H. Jackman (2005), Simulation of the October–November 2003 solar proton events in the CMAM GCM: Comparison with observations, *Geophys. Res. Lett.*, *32*, L15S02, doi:10.1029/2005GL022392.

Seppälä, A., P. T. Verronen, E. Kyrölä, S. Hassinen, L. Backman, A. Hauchecorne, J. L. Bertaux, and D. Fussen (2004), Solar proton events of October–November 2003: Ozone depletion in the Northern Hemisphere polar winter as seen by GOMOS/Envisat, *Geophys. Res. Lett.*, *31*, L19107, doi:10.1029/2004GL021042.

Seppälä, A., P. T. Verronen, V. F. Sofieva, J. Tamminen, E. Kyrölä, C. J. Rodger, and M. A. Clilverd (2006), Destruction of the tertiary ozone maximum during a solar proton event, *Geophys. Res. Lett.*, *33*, L07804, doi:10.1029/2005GL025571.

Seppälä, A., P. T. Verronen, M. A. Clilverd, C. E. Randall, J. Tamminen, V. F. Sofieva, L. Backman, and E. Kyrölä (2007), Arctic and Antarctic polar winter NO_x and energetic particle precipitation in 2002–2006, *Geophys. Res. Lett.*, *34*, L12810, doi:10.1029/2007GL029733.

Seppälä, A., M. A. Clilverd, C. J. Rodger, P. T. Verronen, and E. Turunen (2008), The effects of hard-spectra solar proton events on the middle atmosphere, *J. Geophys. Res.*, *113*, A11311, doi:10.1029/2008JA013517.

Seppälä, A., C. E. Randall, M. A. Clilverd, E. Rozanov, and C. J. Rodger (2009), Geomagnetic activity and polar surface air temperature variability, *J. Geophys. Res.*, *114*, A10312, doi:10.1029/2008JA014029.

Smith, A. K., M. López-Puertas, M. García-Comas, and S. Tukiainen (2009), SABER observations of mesospheric ozone during NH late winter 2002–2009, *Geophys. Res. Lett.*, *36*, L23804, doi:10.1029/2009GL040942.

Smith, A. K., R. R. Rolando, D. R. Marsh, and J. H. Richter (2011), WACCM simulations of the mean circulation and trace species transport in the winter mesosphere, *J. Geophys. Res.*, *116*, D20115, doi:10.1029/2011JD016083.

Sofieva, V. F., N. Kalakoski, P. T. Verronen, S.-M. Päivärinta, E. Kyrölä, L. Backman, and J. Tamminen (2012), Polar-night O_3, NO_2 and NO_3 distributions during sudden stratospheric warmings in 2003–2008 as seen by GOMOS/Envisat, *Atmos. Chem. Phys.*, *12*, 1051–1066, doi:10.5194/acp-12-1051-2012.

Solomon, S., P. J. Crutzen, and R. G. Roble (1982), Photochemical coupling between the thermosphere and the lower atmosphere 1. Odd nitrogen from 50 to 120 km, *J. Geophys. Res.*, *87*, 7206–7220.

Turunen, E., P. T. Verronen, A. Seppälä, C. J. Rodger, M. A. Clilverd, J. Tamminen, C.-F. Enell, and T. Ulich (2009), Impact of different precipitation energies on NO_x generation during geomagnetic storms, *J. Atmos. Sol. Terr. Phys.*, *71*, 1176–1189, doi:10.1016/j.jastp.2008.07.005.

Verronen, P. T., A. Seppälä, M. A. Clilverd, C. J. Rodger, E. Kyrölä, C.-F. Enell, T. Ulich, and E. Turunen (2005), Diurnal variation of ozone depletion during the October–November 2003 solar proton events, *J. Geophys. Res.*, *110*, A09S32, doi:10.1029/2004JA010932.

Verronen, P. T., A. Seppälä, E. Kyrölä, J. Tamminen, H. M. Pickett, and E. Turunen (2006), Production of odd hydrogen in the mesosphere during the January 2005 solar proton event, *Geophys. Res. Lett.*, *33*, L24811, doi:10.1029/2006GL028115.

von Clarmann, T., B. Funke, M. López-Puertas, S. Kellmann, A. Linden, G. P. Stiller, C. H. Jackman, and V. L. Harvey (2013), The solar proton events in 2012 as observed by MIPAS, *Geophys. Res. Lett.*, doi:10.1002/grl.50119.

Waters, J. W., et al. (2006), The Earth Observing System Microwave Limb Sounder (EOS MLS) on the Aura satellite, *IEEE Trans. Geosci. Remote Sens.*, *44*, 1075–1092, doi:10.1109/TGRS.2006.873771.